Atmospheric Environment 96 (2014) 145–153

Contents lists available at ScienceDirect

Atmospheric Environment

journal homepage: www.elsevier.com/locate/atmosenv

Atmospheric chemistry of HFE-7300 and HFE-7500: Temperature dependent kinetics, atmospheric lifetimes, infrared spectra and global warming potentials

Ana Rodríguez [a, *], Diana Rodríguez [a], Araceli Moraleda [a], Iván Bravo [b], Elena Moreno [c], Alberto Notario [d]

[a] Faculty of Environmental Sciences and Biochemistry, University of Castilla La Mancha, Avenida Carlos III, s/n, 45071 Toledo, Spain
[b] Faculty of Pharmacy, Physical Chemistry Department, University of Castilla La Mancha, Campus de Albacete, Edificio Polivalente, s/n, 02071 Albacete, Spain
[c] Institute of Structure of Matter, Molecular Physics Department, CSIC, Serrano 121, 28006 Madrid, Spain
[d] Faculty of Chemical Sciences, University of Castilla La Mancha, Avenida Camilo José Cela 10, 13071 Ciudad Real, Spain

HIGHLIGHTS

- Atmospheric lifetimes and reaction mechanisms of HFE-7300 and HFE-7500 were elucidated.
- Infrared spectra have been measured and radiative forcing efficiencies and global warming potentials were determined.
- These results enable the discussion of the environmental compatibility of HFE-7300 and HFE-7500.

GRAPHICAL ABSTRACT

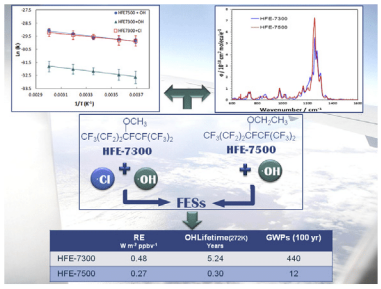

ARTICLE INFO

Article history:
Received 28 March 2014
Received in revised form
7 July 2014
Accepted 14 July 2014
Available online 15 July 2014

Keywords:
HFE-7300
HFE-7500
Atmospheric lifetimes
Reaction mechanism
Infrared spectra
Radiative efficiencies

ABSTRACT

The atmospheric degradation of two hydrofluoroethers, HFE-7300 [n-$C_2F_5CF(OCH_3)CF(CF_3)_2$] and HFE-7500 [$n$-$C_3F_7CF(OC_2H_5)CF(CF_3)_2$] used in industrial applications has been studied. The kinetics and reaction products were determined at atmospheric pressure as a function of temperature in a reaction chamber using GC/FID and GC/MS techniques for the analysis. The following Arrhenius expressions were obtained (in units of cm^3 $molecule^{-1}$ s^{-1}): $k_{HFE\text{-}7300\ +\ OH} = (5.6 \pm 2.0) \times 10^{-13} \exp(-(1186 \pm 111)/T)$; $k_{HFE\text{-}7300\ +\ Cl} = (3.8 \pm 1.3) \times 10^{-12} \exp(-(968 \pm 101)/T)$; and $k_{HFE\text{-}7500\ +\ OH} = (7.6 \pm 6.0) \times 10^{-12} \exp(-(1163 \pm 385)/T)$ (temperature range 271–333 K). The atmospheric lifetimes calculated from kinetic data for HFE-7300 and HFE-7500 were 5.24 and 0.30 years, respectively. In the oxidation of HFE-7300 with OH and Cl radicals, the only detected product was $CF_3CF_2CF(OCHO)CF(CF_3)_2$, whereas in the oxidation of HFE-7500 by OH radicals the detected products were: $C_3F_7CF(OC(O)CH_3)CF(CF_3)_2$ and $C_3F_7CF(OC(O)H)CF(CF_3)_2$. Infrared spectra of the studied HFEs have also been measured and radiative forcing efficiencies were determined. Combining these results with the kinetic data, we estimated 100-year time horizon global warming potentials of 440 and 12 for HFE-7300 and HFE-7500, respectively.

* Corresponding author.
E-mail address: [redacted]@uclm.es (A. Rodríguez).

http://dx.doi.org/10.1016/j.atmosenv.2014.07.033
1352-2310/

1. Introduction

The adverse environmental impact of chlorinated hydrocarbons on the Earth' ozone layer (Molina and Rowland, 1974; Farman et al., 1985) has focused attention on the effort to replace these compounds with environmentally acceptable substitutes. Hydrofluoroethers (HFEs) have been developed as new alternatives to replace chlorofluorocarbons (CFCs), hydrochlorofluorocarbons (HCFCs) and hydrofluorocarbons (HFCs) in applications such as refrigerants, blowing and cleaning agents, and they are also used as fuels additives, solvents, and medical products (Tsai, 2005). HFE-7300 [n-$C_2F_5CF(OCH_3)CF(CF_3)_2$] and HFE-7500 [$n$-$C_3F_7CF(OC_2H_5)CF(CF_3)_2$] are members of this class of compounds. Thus, HFE-7500 shares many of the inertness and dielectric properties of perfluorinated fluids, and is expected to offer superior environmental behavior. HFE-7300 is effective at mitigating the aggressiveness of solvents and the flammability of blends (3M™ Novec™ 7500 Engineered Fluid). HFE-7300 and 7500 are volatile liquids with a vapor pressure of 5.9×10^6 and 2.1×10^3 Pa at 25 °C (3M™ Novec™ 7500 Engineered Fluid), respectively, which will be released into the atmosphere during their use. In this sense, it is necessary to perform tropospheric kinetic and product studies of these HFEs, in order to assess the impact of their degradation processes on the air quality and global warming.

Generally, HFEs show low surface sticking coefficients and low water solubility. Thus, primary removal of HFEs in the troposphere will mainly be initiated by reaction with OH radicals. Although global atmospheric abundance of OH radical is around 3 orders of magnitude greater than that of chlorine atoms, Cl reactions are generally faster than OH reactions, so their contribution to the degradation of organic compounds may be not negligible compared to the role of OH (Finlayson-Pitts and Pitts, 2000). The contribution of Cl atoms to the oxidation of HFEs could be significant in areas where the concentration of chlorine precursor species has been reported to be high. Thus, Cl atom initiated oxidation may have a significant local impact for very short-lived substances (VSLS) – lifetimes less than a few months – in those areas (WMO, 2011). In this sense, recent studies suggest that in the early morning, the production rate of the Cl atoms exceeds the production of OH radicals for 2–3 h after sunrise, when high concentrations of $ClNO_2$, precursor of the atoms of chlorine through its photolysis, have been measured in different parts of the world (Osthoff et al., 2008; Thornton et al., 2010; Mielke et al., 2011; Phillips et al., 2012).

The tropospheric lifetimes for most gases are generally controlled by reactions with OH radicals (Kurylo and Orkin, 2003). However, reactions with other oxidants as Cl radical can also play limited roles. The calculation of atmospheric lifetimes is complicated due several sources as the temporal and spatial variability of the reacting species concentrations what lead to the difficulty to be confident of their absolute concentrations. Besides, accurate determinations of the temperature-dependent rate coefficients with tropospheric oxidants, as OH and Cl, are essentials due the negative vertical temperature profile of the troposphere. In this sense, chemical species of low reactivity will possess lifetimes larger that the characteristic mixing time in the troposphere and will present a relatively homogeneous vertical distribution therein (well-mixed compounds). On the other hand, there are no unique lifetimes for VSLS since they are not "well-mixed" and their lifetimes depends, on the altitude and latitude of emissions along with the chemical and physics conditions of the atmosphere. Therefore, temperature-dependence rate coefficient studies of the reactions of emitted species with atmospheric oxidant are crucial to obtain accurate values for atmospheric lifetimes (WMO, 2011).

In this work we report the first study of the temperature dependence of the kinetics of the reactions of OH radicals with HFE-7300 and HFE-7500, and Cl atoms with HFE-7300. To our knowledge, there is only a single previous kinetic study on the OH + HFE-7500 reaction at room temperature and low pressure (Goto et al., 2002). It is also here presented the first, as far as we know, experimental study on the degradation pathways and yields of the aforementioned reactions. This work is also the first to report infrared absorption cross section spectra for HFE-7300 and HFE-7500 (for HFE-7500 only absorption spectrum was available (Goto et al., 2002)). Using the Pinnock et al. (1995) method together with the spectral data we have estimated the radiative forcing efficiencies. Finally, combining these parameters with kinetic data we have obtained the corresponding global warming potential values; the results enable the discussion of the environmental compatibility of HFE-7300 and HFE-7500.

2. Experimental

2.1. Kinetic study

The experimental system used in this study has been previously described in detail (Rodríguez et al., 2010), therefore, only a brief description is given here. Relative-rate experiments were carried out in a 400 L Teflon bag housed in an isothermal cabinet with 6 fluorescent lamps mounted on the walls. The experiments were performed within the temperature range of 271–333 K at ∽760 torr of total pressure of N_2 or synthetic air. Cl and OH radicals were generated by photolysis of Cl_2 and H_2O_2, at $\lambda_{max} = 360$ nm and $\lambda_{max} = 254$ nm, respectively. In the smog chamber experiments, the unwanted loss of reactants and products via photolysis, dark chemistry and heterogeneous reactions have to be considered. In this sense, the loss rate was negligible compared to the rate of reaction in all cases.

Kinetic data were derived by monitoring the loss of the HFE relative to one or more reference compounds:

$$Cl/OH + HFE \rightarrow Products \quad k_{HFE}$$

$$Cl/OH + Reference \rightarrow Products \quad k_R$$

The decays of the reactant and reference were then plotted using the expression:

$$Ln\frac{[HFE]_0}{[HFE]_0} = \frac{k_{HFE}}{k_R} Ln\frac{[Reference]_0}{[Reference]_t} \quad (I)$$

where $[HFE]_{t0}$, $[HFE]_t$, $[Reference]_{t0}$, and $[Reference]_t$ are the concentrations at times 0 and t, and k_{HFE} and k_R are the rate constants for the reactions of the hydrofluoroethers and the reference compound with Cl or OH radicals, respectively. Plots of $Ln([HFE]_0/[HFE]_t)$ vs. $Ln([Reference]_0/[Reference]_t)$ should be linear, pass through the origin and have a slope equal to k_{HFE}/k_R.

The decay of HFE and reference compound was monitored by gas chromatography, with flame ionization detection, GC–FID (Shimadzu 2010), using a capillary column (size: 30 m × 0.32 mm × 1 μm. Meta.X5 Teknokroma) maintained isothermal at 40 °C. The concentration ranges of the reactants were as follow: (in molecule cm^{-3}): HFE $(4.2–9.6) \times 10^{14}$, reference compound $(1.5–6.4) \times 10^{15}$, H_2O_2 $(4.7–18.4) \times 10^{15}$ and Cl_2 $(4.2–5.6) \times 10^{15}$ (see Table 1S, in Supporting information). For each mixture of organic compounds, a number of injections of the unreacted mixture, usually 10 or more, were carried out in order to obtain an estimate of the precision associated with the measurements, and to be used in the error analysis. The standard deviations (2σ) of these replicate injections were typically 1–2% for both HFEs and reference compounds.

2.2. Product study

The products formed in the reactions of Cl or OH radicals with the studied HFEs were measured by GC–mass spectrometry (Shimadzu QP2010) for their identification, and by GC–FID for their quantification. The temperature program used in both chromatographs on a 30 m Meta.X5 column was the following: 40 °C (8 min), 10 °C/min to 100 °C and hold 3 min. All experiments were carried out in the absence and presence of NOx, with initial reactant concentrations as follow: (in molecule cm^{-3}): HFE (3.4–7.8) × 10^{14}, H_2O_2 (1.5–4.1) × 10^{15}, Cl_2 (2.8–4.2) × 10^{15} and NO (1.2–2.4) × 10^{15}. The identification of the products was made by analysis of the mass spectrum. In order to determine the concentrations of the HFE and the detected products, the GC–FID response factors of each compound were determined by introducing different known amounts of the commercial sample into the Teflon chamber and conducting several replicate analyses. Product yields were obtained from plots of the amount of the detected product against the amount of lost reactant. For compounds that are not commercially available, the yields were estimated using the effective carbon number method, ECN (Scanlon and Willis, 1985).

2.3. Infrared spectra

Infrared spectra of HFE-7300 and HFE-7500 were measured in our laboratory. Measurements were obtained at 298 K using a 50 L quartz-glass reactor equipped with a White-type multiple-reflection mirror system with a base length of 1.37 m and a total optical path length of 197 m. Details of the experimental set-up can be found elsewhere (Bravo et al., 2013) (see Supporting information as well). The IR spectra were obtained by co-adding 64 scans with a resolution of 1 cm^{-1} in the spectral range 2000–600 cm^{-1}, using a Bruker, VERTEX 80V FTIR spectrophotometer, equipped with a MCT (mercury cadmium telluride) detector. The compounds were injected into the reactor at concentrations within (0.4–5) × 10^{13} molecule cm^{-3}, and mixed there with synthetic air to a total pressure within (25–150) ± 2 torr.

To ensure that saturation was not a problem in the measurements, for each compound, the peak absorbance was plotted as function of pressure. Points at higher pressures showing non-linear behavior were ignored. Plots of absorbance vs. compound concentration showed good linearity, and zero intercepts (see Fig. S1, Supporting information). The spectra were then normalized to this value for the cross section and the integrated absorption cross section calculated from the average of the spectra.

No dependence on total pressure was observed for both studied compounds. The cross section spectra presented here were calculated from the average of the cross section spectra measured within 25–70 torr (we discarded measurements within 70–150 torr because of the noise).

Absorption and integrated absorption cross section of HFE-7300 and HFE-7500 at 298 K were then obtained using the corresponding relationships described in literature (Bravo et al., 2013).

2.4. Reagents

The chemicals used and their stated purities were as follows: HFE-7300 (>99.5%, 3 M), HFE-7500 (>99%, 3 M), Cl_2 (>99,8%, Praxair), hydrogen peroxide (>60%, Fisher Chemical), methane (99%, Air Liquide), chloromethane (99.5%, Aldrich), dichloromethane (>99%, Fluka), ethane (>99%, Aldrich), chloroethane (99.7%, Aldrich) and methyl perfluorooctanoate (98%, Aldrich). Synthetic air (99.999%, Air Liquide) and N_2 (99.999%, Air Liquide) were employed as bath gases for the experiments, and He (99.998%, Air Liquide) was used as GC carrier gas.

3. Results and discussion

3.1. Kinetic study

The kinetic studies of degradation of HFE-7300 with OH and Cl radicals and HFE-7500 with OH radicals were carried out at atmospheric pressure within the temperature range 271–333 K.

Fig. 1 shows the loss of the title HFEs vs. the reference compounds following exposure to OH or Cl radicals at 298 ± 1 K and ~760 torr of air or N_2. Consistently with expectations (Eq. (I)), the plots were linear with zero intercept.

The reference compounds used in this study were methane, chloromethane, dichloromethane, ethane and chloroethane whose rate constants with OH radicals are as follow: (3.6 ± 0.4) × 10^{-14} cm^3 $molecule^{-1}$ s^{-1} and (1.0 ± 0.1) × 10^{-13} cm^3 $molecule^{-1}$ s^{-1} for chloromethane and dichloromethane respectively (Atkinson et al., 2008); (2.4 ± 0.2) × 10^{-13} cm^3 molecule^{-1} s^{-1} for ethane (Atkinson et al., 2006); and (4.2 ± 0.4) × 10^{-13} cm^3 $molecule^{-1}$ s^{-1} for chloroethane (Cohen and Westberg, 1991). The rate constants of the reactions of Cl atoms with the compounds used as reference were taken from the values reported by Atkinson et al.: (1.0 ± 0.1) × 10^{-13} cm^3 $molecule^{-1}$ s^{-1} for methane (Atkinson et al., 2006) and (4.8 ± 0.5) × 10^{-13} cm^3 $molecule^{-1}$ s^{-1} and (3.4 ± 0.3) × 10^{-13} cm^3 $molecule^{-1}$ s^{-1} for chloromethane and dichloromethane (Atkinson et al., 2008), respectively.

A linear least-square analysis of the relative rate plots gives the following rate constants (in units of cm^3 $molecule^{-1}$ s^{-1} and errors ± 2σ): $k_{HFE\text{-}7300\ +\ OH}$ = (1.10 ± 0.35) × 10^{-14}, $k_{HFE\text{-}7300\ +\ Cl}$ = (1.50 ± 0.30) × 10^{-13} and $k_{HFE\text{-}7500\ +\ OH}$ = (1.37 ± 0.29) × 10^{-13}, which are the average of the individual determinations with various reference compounds and air or N_2 as bath gases (see more detailed information in Table S1, Supporting information). The obtained results were independent of the bath gas used, so the absence of changes due to the presence of O_2 suggests that there is no interference from secondary reactions (Kaiser and Wallington, 1996).

For all the studied reactions, the rate constants were found to increase with increasing temperature, as shown in Fig. 2 in the form of Arrhenius plots. The rate constants were measured over the range 271–333 K at atmospheric pressure (see Table 2S, Supporting information), using chloromethane as reference compound in the reactions with OH radicals ($k_{CH_3Cl+OH} = (2.1) \times 10^{-12} \exp(-1210\pm 200/T)$$cm^3$ $molecule^{-1}$ s^{-1}) (Atkinson et al., 2008), and dichloromethane in the reaction with Cl atoms ($k_{CH_2Cl_2+Cl} = (5.9) \times 10^{-12}$ $\exp(-850\pm200/T)$$cm^3$ $molecule^{-1}$ s^{-1}) (Atkinson et al., 2008).

The linear weighted least-squares analysis of the data yields the activation energies and the pre-exponential factors, and affords the calculation of the kinetic rate constants through the following equations (errors are ±2σ):

$$k_{HFE-7300+OH} = \left(5.6\pm2.0\right) \times 10^{-13} \times \exp\left(-(1186\pm111)/T\right) cm^3\ molecule^{-1}\ s^{-1}$$

$$k_{HFE-7300+Cl} = \left(3.8\pm1.3\right) \times 10^{-12} \times \exp\left(-(968\pm101)/T\right) cm^3\ molecule^{-1}\ s^{-1}$$

$$k_{HFE-7500+OH} = \left(7.6\pm6.0\right) \times 10^{-12} \times \exp\left(-(1163\pm385)/T\right) cm^3\ molecule^{-1}\ s^{-1}$$

This work reports the first temperature dependence study for the degradation of HFE-7300 with OH and Cl radicals and HFE-7500

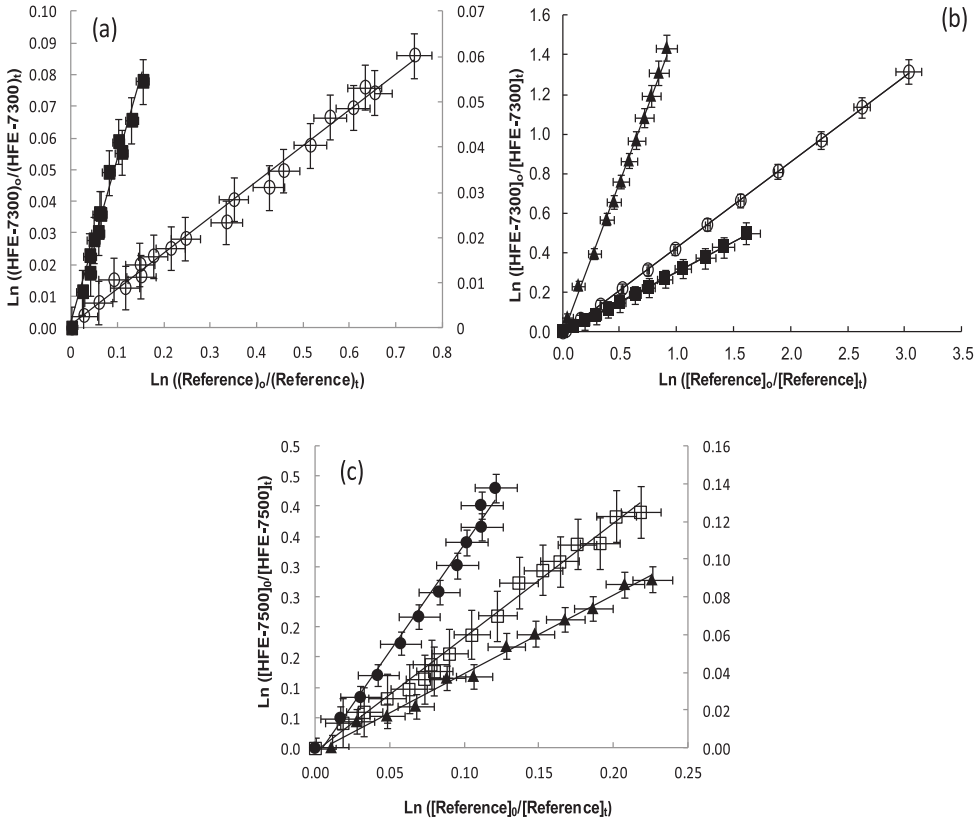

Fig. 1. Relative rate plot at 298 ± 1 K and ~760 torr of the reactions (a) HFE-7300 + OH: Left *y*-axis: Chloromethane (■); Right *y*-axis: Dichloromethane (○) as reference compounds; (b) HFE-7300 + Cl: Methane (▲), Chloromethane (■) and Dichloromethane (○) as reference compounds; (c) HFE-7500 + OH; Left *y*-axis: Chloromethane (●); Right *y*-axis: Ethane (▫) and Chloroethane (▲) as reference compounds.

with OH radicals. There is a single previous study of the kinetic of the reaction of HFE-7500 with OH radicals at room temperature carried out by Goto et al. (2002). These authors studied the HFE-7500 + OH reaction at 295 K and ∽200 torr of total pressure in a relative technique (FTIR–photolysis system), and reported a value of $(2.6 \pm 0.6) \times 10^{-14}$ cm^3 molecule^{-1} s^{-1}. This value is around five times lower than that reported herein (2.6 vs. 13.7×10^{-14} cm^3 molecule^{-1} s^{-1}). This fact may suggest a pressure dependence of the rate constant, however, the H-abstraction reactions of other reported HFEs are usually independent of the total pressure (Bravo et al., 2010a; Díaz-de-Mera et al., 2009), and therefore the source of this discrepancy is not clear. On the other hand, our results are consistent with kinetic rate constant for fluorinated ethers with similar reactive sites in the molecule, as can be shown in Table 1. For instance, HFE-7300 + OH rate constant presented here is in agreement with those found in literature for HFEs with a methyl group in their structure, as $C_3F_7OCH_3$, $(CF_3)_2CFOCH_3$, $C_4F_9OCH_3$ or CF_3OCH_3. A similar comparison can be made for HFE-7500 + OH rate constant presented here with HFEs with a methylene group in their structure, as $CF_3OC_2H_5$ and $C_4F_9OC_2H_5$. Besides, if it is considered the HFE-7300 + Cl reaction, the agreement is also good when we compare to $C_5F_{11}OCH_3$, $C_4F_9OCH_3$, $C_3F_7OCH_3$ and CF_3OCH_3, all of them containing a methyl group in their structures. Therefore, a comparable reactivity is obtained with fluorinated ethers of similar structure, showing that the rate constant is not dependent on the number of $-CF_2-$ in the perfluorinated chain, even though when this chain is branched (Bravo et al., 2010a; Tokuhashi et al., 1999).

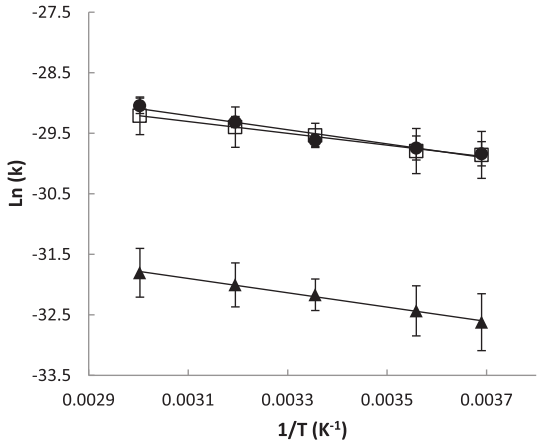

Fig. 2. Arrhenius plots at atmospheric pressure of the reactions: (▲) HFE-7300 + OH; (▫) HFE-7300 + Cl; and (●) HFE-7500 + OH.

On the contrary, the reactivity decrease of the fluorinated ethers compared to non fluorinated ethers presumable reflects the increase in C–H bond strength associated with the presence of multiple fluorinated substituents (Goto et al., 2002; Stein et al., 1991). For instance, in Table 1 we can see that OH rate constant for *n*-$C_4H_9OC_2H_5$ is more than 200 times larger than that found for the corresponding fluorinated ether $C_4F_9OC_2H_5$.

Finally, the replacement of a methyl group in HFE-7300 by an ethyl group in HFE-7500 leads to a substantial reactivity increase towards OH and Cl radicals with $k_{\text{HFE-7500}}$ more than 10 times larger than $k_{\text{HFE-7300}}$ for both radicals: 1.1 vs 13.7×10^{-14} cm^3 molecule^{-1} s^{-1} for OH, and 1.5 vs 22.0×10^{-13} cm^3 molecule^{-1} s^{-1} for Cl (see Table 1). As is

Table 1
Rate constants of the reactions of non-fluorinated ethers and fluorinated ethers with OH and Cl radicals.

	Non fluorinated ether		Fluorinated ether	
	Ether	k (cm^3 $molecule^{-1}$ s^{-1})	HFE	k (cm^3 $molecule^{-1}$ s^{-1})
OH	CH_3OCH_3	2.77×10^{-12}[a]	n-$C_2F_5CF(OCH_3)CF(CF_3)_2$ HFE-7300	1.11×10^{-14}[f]
	$C_2H_5(CH_3)_2OCH_3$	6.08×10^{-12}[b]	$C_3F_7OCH_3$ (HFE-7000)	1.54×10^{-14}[g]
	n-$C_5H_{11}OCH_3$	6.19×10^{-12}[c]	$(CF_3)_2CFOCH_3$	1.52×10^{-14}[h]
	$C_2H_5OC_2H_5$	1.36×10^{-11}[d]	$C_4F_9OCH_3$ (HFE-7100)	1.49×10^{-14}[g]
			CF_3OCH_3 (HFE-143a)	1.19×10^{-14}[i]
	$tert$-$C_4H_9OC_2H_5$	8.80×10^{-12}[c]	n-$C_3F_7CF(OC_2H_5)CF(CF_3)_2$ (HFE-7500)	1.37×10^{-13}[f]
	n-$C_4H_9OC_2H_5$	2.08×10^{-11}[c]	$C_4F_9OC_2H_5$ (HFE-7200)	1.00×10^{-13}[j]
			$CF_3OC_2H_5$ (HFE-263)	1.55×10^{-13}[k]
Cl	CH_3OCH_3	1.30×10^{-10}[e]	n-$C_2F_5CF(OCH_3)CF(CF_3)_2$ HFE-7300	1.50×10^{-13}[f]
			$C_3F_7OCH_3$ (HFE-7000)	1.24×10^{-13}[l]
	$C_4H_9OCH_3$	1.40×10^{-10}[e]	$C_4F_9OCH_3$ (HFE-7100)	1.43×10^{-13}[m]
			$C_5F_{11}OCH_3$	1.03×10^{-13}[n]
			CF_3OCH_3 (HFE-143a)	1.40×10^{-13}[o]
	$C_2H_5OC_2H_5$	2.50×10^{-10}[e]	n-$C_3F_7CF(OC_2H_5)CF(CF_3)_2$ (HFE-7500)	2.20×10^{-12}[p]
	$C_4H_9OC_2H_5$	1.50×10^{-10}[e]	$C_4F_9OC_2H_5$ (HFE-7200)	2.70×10^{-12}[q]

[a] Bonard et al. (2002).
[b] Teton et al. (1995).
[c] Teton et al. (1996).
[d] Mellouki et al. (1995).
[e] Notario et al. (2000).
[f] This work.
[g] Bravo et al. (2010a).
[h] Stein et al. (1991).
[i] Chen et al. (2001).
[j] Oyaro and Nielsen (2003).
[k] Oyaro et al. (2005).
[l] Diaz-de-Mera et al. (2008).
[m] Aranda et al. (2006).
[n] Nohara et al. (2001).
[o] Christensen et al. (1999).
[p] Díaz-de-Mera et al. (2009).
[q] Christense et al. (1998).

summarized in Table 1, this behavior was also observed for other HFEs with similar structure; as e.g. HFE-7200 and HFE-7100, where the rate constant with OH and Cl radicals is larger for HFE-7200 than for HFE-7100 (Bravo et al., 2010a; Aranda et al., 2006). All these observations have interesting implications for the design of chemical structures with particular industrial applications. The length (and branching) of the fluorinated part of the ether may be substantially modified to provide the desired physico-chemical behavior while the alkyl part may be modified to increase the gas-phase reactivity and hence ensure efficient elimination from the troposphere.

3.2. Mechanism of the atmospheric oxidation of HFE-7300

Fig. 3a shows the reaction mechanism proposed for the reaction of HFE-7300 with OH and Cl radicals. The atmospheric degradation of HFE-7300 proceeds through the abstraction of an H atom and the alkyl radical formed in this reaction adds O_2 to form the corresponding alkyl peroxy radical. Depending on the experimental conditions, absence or presence of NOx, the peroxy radicals may react with NO, HO_2, other peroxy radicals or with themselves, giving rise to the corresponding alkoxy radical. This radical can decompose by C–C bond scission or react with O_2, leading to the different reaction products.

Based on the fragmentation pattern from the electron impact mass spectrum (see Fig. S2, Supporting information), the only product detected by the GC–MS instrument in the oxidation of HFE-7300 by OH and Cl radicals was $CF_3CF_2CF(OCHO)CF(CF_3)_2$ (both in presence and absence of NOx). This compound arises from the reaction of the alkoxy radical with O_2. Goto et al. (2002) compared the relative importance of the decomposition channel of the alkoxy radical vs. its reaction with O_2 for fluorinated ethers and non fluorinated ethers. This study suggests that the fluorination of alkoxy radical leads to an increase in the reaction with O_2. Unfortunately, in this work the yield of the fluorinated formate could not be calculated since this product is not commercial and we have not found a compound of similar structure suitable for our experiments.

3.3. Mechanism of the atmospheric oxidation of HFE-7500

Mass spectra of the two products detected in the oxidation of HFE-7500 by OH radicals are the same in the absence and presence of NOx (see Fig. S2, Supporting information). One of the detected products was identified as $C_3F_7CF(OC(O)CH_3)CF(CF_3)_2$, observing an ion signal at $m/z = 43$ typical of the loss $-C(O)CH_3$ group. The mass spectrum of the other detected product shows ion signals at $m/z = 28$ and 29, typical of the loss $-C(O)\cdot$ and $-C(O)H$ (Fig. S2). Taking into account the proposed mechanism, Fig. 3b, two possible compounds can be assigned to this spectrum: $C_3F_7CF(OC(O)H)CF(CF_3)_2$ or $C_3F_7CF(OCH_2C(O)H)CF(CF_3)_2$. Although methylene and the terminal methyl groups are both susceptible of H-abstraction, generally, OH and Cl radicals react faster through the abstraction of the most weakly bound hydrogen atoms in the molecule. In this sense, a previous theoretical work involving hydrofluoroethers (Papadimitrou et al., 2004) has shown that H–C bonds are weaker in $-CH_2$ groups than those of $-CH_3$ groups. Furthermore, experimental studies of Cl and OH reactions with $C_4F_9OC_2H_5$ (HFE-7200) (Aranda et al., 2006; Christense et al., 1998) showed that the preferred site of reaction was the $-CH_2$ position. Thus, the detected product arises probably of reaction on the $-CH_2$ group and corresponds to the fluorinated formate: $C_3F_7CF(OC(O)H)CF(CF_3)_2$. Similar results were found in the study of the reaction of HFE-7500 with Cl atoms where the fluorinated acetate was found as the major

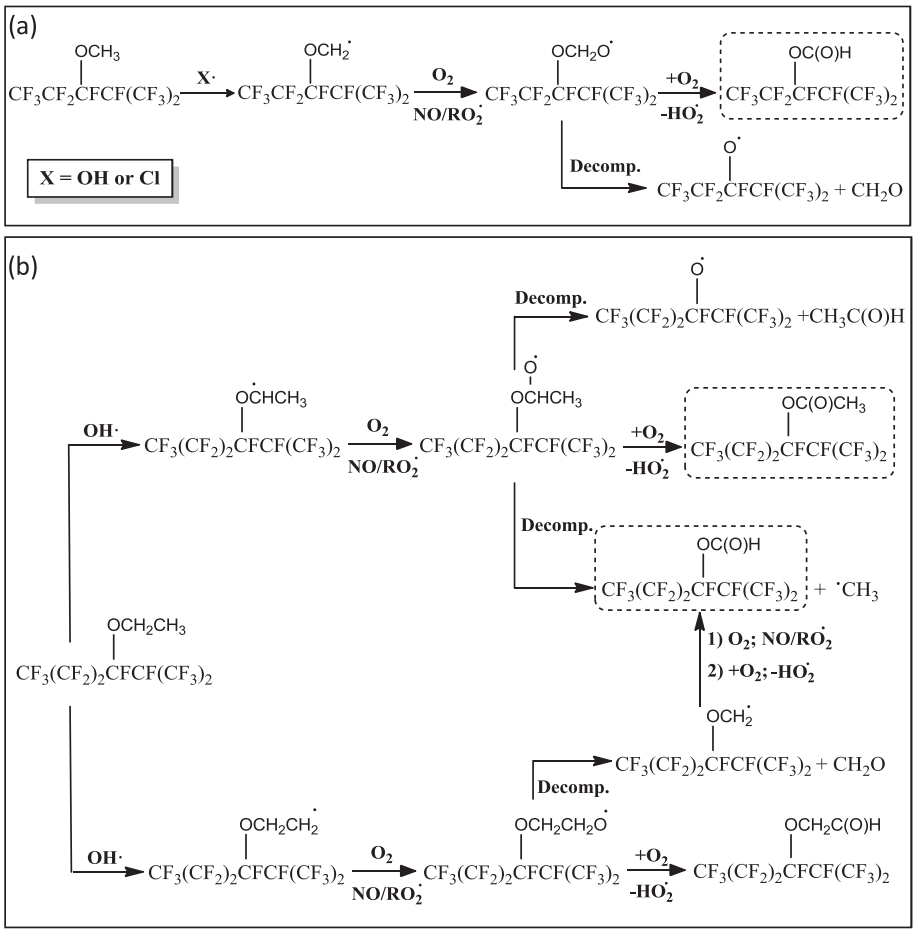

Fig. 3. Proposed mechanisms for the reactions of (a) HFE-7300 with OH or Cl radicals (X) and (b) HFE-7500 + OH; where the detected products are shown in dashed box.

product and the fluorinated formate was reported as a minor product (Goto et al., 2002).

Even though the fluorinated acetate, $C_3F_7CF(OC(O)CH_3)CF(CF_3)_2$, is not commercially available, its yield was estimated from the calibration of a compound with the same molecular formula and commercially available, methyl perfluorooctanoate, using the ECN method (Scanlon and Willis, 1985) (see Fig. S3, Supporting information). The molar yields in the absence and presence of NOx were (59 ± 8%) and (49 ± 9%), respectively. The total error is a combination of systematic errors and the uncertainty of ECN method. These yields were calculated from conversion data below 20% to avoid secondary chemistry contributions. As shown, the yield of this acetate decreased in presence of NOx. This difference can be explained by chemical activation effects in the atmospheric chemistry of different alkoxy radicals, that is to say the differences in the exothermicities of the reactions producing the alkoxy radicals. Peroxy radical self-reactions are generally thermoneutral, while the reactions of peroxy radicals with NO are very exothermic. Thus, the alkoxy radicals (RO•) formed by the reaction between RO_2• and NO will have higher internal excitation energy and rapid decomposition of these activated alkoxy radicals through C–C bond rupture can compete effectively with collisional thermalization of the radicals. On contrary, the alkoxy radicals formed in the self-reaction of peroxy radicals (RO_2•) will have little or no excitation energy, and reactions of the radical with O_2 become effective, increasing the acetate yield (Hurley et al., 2009; Blanco et al., 2012). Unfortunately, the yield of the other detected product, tentatively considered as the fluorinated formate obtained from decomposition channel, could not be calculated since this compound is not commercially available and we have not found any available chemical of similar structure suitable to apply the ECN method.

On the other hand, the yield of $C_3F_7CF(OC(O)CH_3)CF(CF_3)_2$ from the reaction of HFE-7500 with Cl has been calculated by Goto et al. (2002). These authors estimate that ∽68% the alkoxy radicals react with O_2 to give the fluorinated acetate. This result is consistent with the yield determined in this work for the fluorinated acetate obtained by OH radical-initiated oxidation (59 ± 8%). In addition, we have to consider that HFE-7500 oxidation may occur at high altitudes and low temperatures in the atmosphere; and, as the decomposition reaction of the alkoxy radical have probably a substantial activation barrier (Goto et al., 2002), a temperature decrease may cause an increase of the yield of the fluorinated acetate in detriment of the fluorinated formate.

3.4. Atmospheric lifetimes

For well-mixed compounds – lifetimes greater than a few months – OH-lifetimes are estimated relative to the corresponding lifetime of methyl chloroform (MCF) at 272 K (see WMO, 2011; Spivakovsky et al., 2000 and Hodnebrog et al., 2013 for further detailed discussion):

$$\tau_{OH(272\ K)} = \frac{k_{OH}^{CH_3CCl_3}(272\ K)}{k_{OH}(272\ K)}\tau_{OH}^{CH_3CCl_3} \qquad (II)$$

where τ_{OH} and $\tau_{OH}^{CH_3CCl_3}$ (=6.1 year[6]) are the lifetimes of a given compound and CH_3CCl_3, respectively, due to the reactions with OH radicals in the troposphere; $k_{OH}(272\ K)$ and $k_{OH}^{CH_3CCl_3}(272\ K)$ (=6.1 ×

10^{-15} cm^3 molecule^{-1} s^{-1} (Sander et al., 2011)) are the rate constants for the reactions of these compounds with OH at 272 K. From the data reported in this work for the rate constants and the Arrhenius expressions, the atmospheric lifetimes can be obtained for HFE-7300 and HFE-7500 at 272 K with OH radicals, from equation II. We found lifetimes of 5.24 and 0.37 years for HFE-7300 and HFE-7500, respectively. Since the characteristic mixing time in the troposphere is around 0.5 years, HFE-7300 may be a well-mixed compound, and the lifetime presented here can be considered to be a global lifetime. On the other hand, HFE-7500 is far from being homogeneously distributed and may be considered a VSLS. As was briefly mentioned before, the lifetime for HFE-7500 may depends on when and where the compound is emitted along with the atmosphere conditions (see WMO, 2011). To be consisted with the methodology described by WMO, 2011 for VSLS, we used $\tau = 1/k(275\ \mathrm{K})[\mathrm{OH}]$ and a global average concentrations [OH] = 1×10^6 molecules cm^{-3} (Prinn et al., 2001) at 275 K for determine an approximate local lifetime of 0.30 years for HFE-7500. Our recommended atmospheric lifetimes for HFE-7300 and HFE-7500 are therefore, 5.24 and 0.30 years, respectively (see Table 2).

In order to compare the relative contributions of OH and Cl radicals assuming a global basic reactive removal process, we also determined the lifetimes of the studied compounds at 298 K. We used $\tau = 1/k_{298}[\mathrm{oxidant}]$ and a global average concentrations of 1×10^6 molecules cm^{-3} (Prinn et al., 2001) and 1×10^3 molecules cm^{-3} (Rudolph et al., 1996) for OH and Cl, respectively (See Table 2). It is clear from the estimated lifetime at 298 K that reactions with OH will play a major role in the atmospheric destruction of the studied HFEs during the day, although the reaction with Cl atoms could also be locally competitive, particularly for HFE-7500.

Lifetime obtained here for HFE-7300 and HFE-7500, evidence that these materials are relatively short-lived and their contribution to the warming may be low even though they are highly fluorinated. In this sense, atmospheric lifetime plays an important role in the determination of the radiative efficiency and global warming potentials. As they depend on the atmospheric compound location, a unique radiative efficiency cannot be defined for very short-lived compounds without a detailed knowledge of the spatial and temporal emission pattern (see section 3.6).

3.5. Infrared absorption cross-section measurements

Infrared spectra for HFE-7300 and HFE-7500 are illustrated in Fig. 4 (cross-section data are summarized in the Supporting information). As expected, all spectra show strong bands at the C–F stretching region within the 1200–1300 cm^{-1} range.

Integrating the spectra between 600 and 2000 cm^{-1} gives the integrated absorption cross sections listed in Table 2. To our knowledge, here we present the first cross section spectrum recorded for HFE-7300. For HFE-7500, Goto et al. (2002) showed the absorption spectra for this molecule but it was not converted into cross section. Therefore, here we present the first data of integrated cross section for the related compound.

As was expected, HFE-7500 shows a stronger absorption than HFE-7300 due the presence of more number of C–F bond in the molecule – with maximum absorption cross section in the region $7–8 \times 10^{-18}$ cm^2 molecule^{-1} – what lead to a larger integrated cross section (46.1 vs. 50.5×10^{-17} cm^2 molecule^{-1} cm^{-1}).

3.6. Radiative forcing efficiencies and global warming potentials

To assess the impact of the release to the atmosphere of HFE-7300 and HFE-7500 has on the radiation budge, and hence in the context to evaluate the climate impact of emission of these gases, the radiative forcing efficiencies (REs) have been calculated using the methodology described by Pinnock et al. (1995) along with the updated 1 cm^{-1} resolution radiative forcing function recently presented by Hodnebrog et al. (2013). In Table 2 we report the REs results assuming perfect mixing. However, the HFEs studied here present relatively short lifetimes, as was commented in section 3.4, and are unlikely to be well-mixed (mainly HFE-7500). Therefore, their mixing ratio will probably fall off rapidly in the stratosphere, and the use of lifetime-correction methodology in the calculation of REs will be necessary. Here we use the recently described S-shaped lifetime-correction proposed by Hodnebrog et al. (2013) for lifetimes within 10^{-4}–10^4 years. This was based on an S-shaped fit to chemical-transport model calculations to crudely account for the fact that short-lived gases are not well-mixed in the atmosphere. The "well-mixed" RE value is multiplied by a factor $2.962\tau^{0.9312}/1 + 2.994\tau^{0.9302}$., where τ is the atmospheric lifetime in years.

"Well-mixed" and lifetime-corrected RE values are summarized in Table 2. Up to our knowledge, we present the first RE literature data for HFE-7300: 0.52 and 0.48 (in W m^{-2} ppbv^{-1}) for "well-mixed" and lifetime-corrected REs, respectively.

For HFE-7500, only the experimental data reported by Goto et al. (2002) was found in literature (0.37 W m^{-2} ppbv^{-1}). This value was calculated using the Pinnock et al. (1995) method without lifetime-correction within the 900–1900 cm^{-1} range. Here we obtained values of 0.56 and 0.27 (in W m^{-2} ppbv^{-1}) for well-mixed and lifetime-corrected REs, respectively (see Table 2). Using the outdated radiative forcing function by Pinnock to compare with Goto et al. data, we obtained a well-mixed RE value for HFE-

Table 2
Atmospheric lifetimes, integrated Absorption Cross Sections (S), Radiative Forcing Efficiencies (RE) — for a constant mixing ratio profile and lifetime-corrected — and GWPs relative to CO_2, for HFE-7300 and HFE-7500. As is recommended by Hodnebrog et al. (2013), we considered an increase of 10% due to stratospheric temperature adjustment for the RE calculations. For the GWP calculations we used the lifetime corrected REs along with the updated values of AGWP for CO_2 presented by Hodnebrog et al. (2013) 2.495×10^{-14}, 9.171×10^{-14} and 32.17×10^{-14} W m^{-2} yr (kgCO_2)$^{-1}$ for time horizons of 20, 100 and 500 years, respectively.

	$\tau_{(298\ \mathrm{K})}$[a] year	Recommended lifetime (τ)[b]/year	S[c,e]	RE[d]	Lifetime corrected RE[d]	GWPs		
						20 yr	100 yr	500 yr
HFE-7300								
OH	2.96	5.24	46.1	0.52	0.48	1620	440	126
Cl	211.40							
HFE-7500								
OH	0.23	0.30	50.5	0.56	0.27	45		3
Cl	14.41					12		

[a] τ (298 K) = $1/k_x$[X] where X = OH or Cl and k_x were obtained from this work and Díaz-de-Mera et al. (2009).
[b] Lifetime calculation is detailed in the text.
[c] Units are 10^{-17} cm^2 molecule^{-1} cm^{-1}.
[d] Units are W m^{-2} ppbv^{-1}.
[e] 600–2000 cm^{-1} and 298 K.

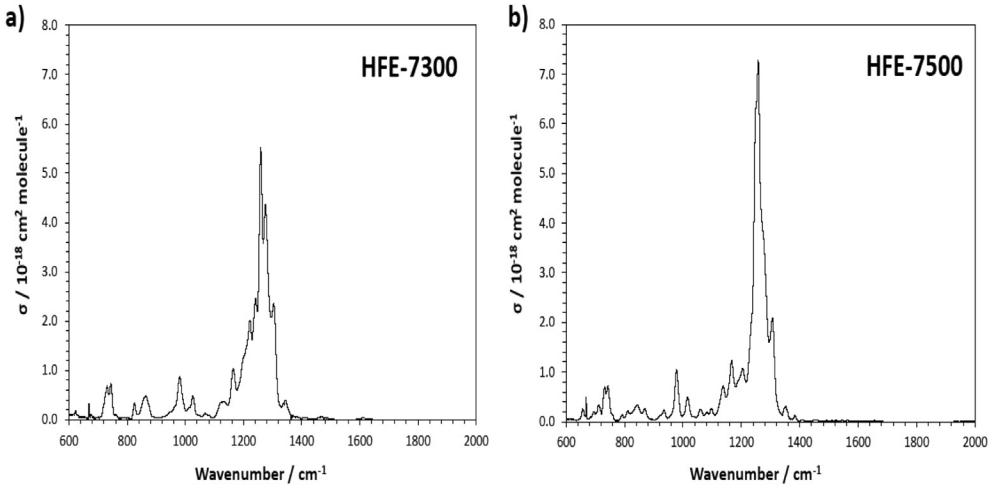

Fig. 4. Infrared spectra of: (a) HFE-7300 and (b) HFE-7500. Spectra have been smoothed to ca. 2 cm^{-1} resolution using a sliding average method.

7500 of 0.54 (in W m^{-2} $ppbv^{-1}$). This value is 31% larger than that obtained by Goto et al.: 0.54 vs. 0.37 (in W m^{-2} $ppbv^{-1}$). This discrepancy may come from the restricted wavenumber interval used for the RE calculation for Goto et al. compared to that used in the present work since the radiative forcing function is strong within 700–900 cm^{-1} (Pinnock et al., 1995). To clarify, we have calculated the RE within 900–1900 cm^{-1} range and we found that our value was still 16% larger than that reported by Goto et al. (2002) (0.44 vs. 0.37 W m^{-2} $ppbv^{-1}$). Differences within 14–25% of existing experimental values provide a valuable data for the REs (Blowers et al., 2007; Bravo et al., 2010b), however, a discrepancy of 16% is high when the same Pinnock's method was used in both studies. Besides, the RE value reported by Goto et al. (2002) for HFE-7500 (n-$C_3F_7CF(OC_2H_5)CF(CF_3)_2$) is surprisingly low when compared to HFEs of the same series but with a lower number of C–F bonds. For instance, the reported RE value for HFE-7200 ($C_4F_9CO_2H_5$) is 0.42 W m^{-2} $ppbv^{-1}$ (Bravo et al., 2010a).

Theoretical methods for the determination of REs may be useful this time to investigate where the discrepancies come from. In this sense, we used the methodology described by Bravo et al. (2010b, 2011a) to determine the RE of HFE-7500. Using this approaching we found REs of 0.55 and 0.43 W m^{-2} $ppbv^{-1}$ for the 0–2500 and 900–1900 cm^{-1} wavenumber intervals, respectively, which are in excellent agreement with the experimental values presented here for well-mixed REs: 0.54 and 0.44 W m^{-2} $ppbv^{-1}$ for the 600–2000 and 900–1900 cm^{-1} intervals respectively. Therefore, it is unclear why the RE obtained by Goto et al. (2002) is lower; this might reflect differences in the spectral variation of the absorption cross-section they used.

The global warming potential (GWP) of a greenhouse gas takes into account both the lifetime and the RE of the gas and represents its contribution to the warming compared to carbon dioxide. The 100 year GWP is the common scale generally used and IPCC (see e.g. Forster et al., 2007) regularly report 20, 100 and 500 year GWP values for a large number of gases. Table 2 presents the 20, 100 and 500 year GWPs obtained here for HFE-7300 and HFE-7500. Note that these values were calculated using the OH lifetimes at 272 K obtained in section 3.4 and lifetime corrected RE values given above to get more realistic results. We can see that the 100 year GWP is considerably higher than that of CO_2 for both gases, particularly for HFE-7300 because of its longer lifetime. However, these values are much smaller than those of the most common CFCs that HFEs use to replace — for instance, the 100 year GWP for CFC-11 is 4660 (Hodnebrog et al., 2013). Here we report the first GWP values for HFE-7300. For HFE-7500, Goto et al. (2002) reported values of GWP relatives to CFC-11 instead of CO_2. When it is converted into GWP relative to CO_2 using the RE and lifetime values they reported for HFE-7500 (2.2 years and 0.37 W m^{-2} $ppbv^{-1}$), leads to a 100 year GWP for HFE-7500 of 110 – almost 10 time larger than that reported herein. Therefore, we consider the GWP values obtained in the present work for HFE-7500 are also the first data currently reported in literature.

To conclude, we have carefully examined the atmospheric lifetimes and REs along with the GWP values derived, and therefore we recommend the data presented here for HFE-7300 and HFE-7500 are the best currently available.

3.7. Atmospheric implications

Proposed H-abstraction mechanisms described in Fig. 3 suggest that oxidation of HFE-7300 and HFE-7500 leads to the corresponding fluorinated ester. According with its short atmospheric lifetime (0.30 year), HFE-7500 rapidly reacts with OH or Cl radicals in the troposphere leading to the corresponding fluorinated formate ($C_3F_7CF(OC(O)H)CF(CF_3)_2$) and acetate ($C_3F_7CF(OC(O)CH_3)CF(CF_3)_2$). As shown in section 3.3, the acetate is presumed to be the main oxidation product, while the remainder could decompose to give the fluorinated formate. Because of its short lifetimes, HFE-7500 may be involved in local smog processes.

On the other hand, HFE-7300 possess a larger atmospheric lifetime compared to HFE-7500, which suggests that it may remain in the troposphere for a longer time while its oxidation with OH and Cl occurs. As commented in section 3.2, the corresponding fluorinated formate ($C_2F_5CF(OCHO)CF(CF_3)_2$) is supposed to be the unique direct oxidation product because of the presence of the $-CH_3$ group in the structure.

GWP values presented in section 3.6 are direct-GWP, which take into account only the direct effect of the emitted compound. Nevertheless, fluorinated formates and acetates are potentially greenhouse gases since they absorb infrared radiation strongly within the atmospheric windows, due to the presence of C–F bonds in the molecule. Many fluorinated esters contribute more actively to global warming than the parent HFEs, even when they both have the same number of C–F bonds in the molecular structure (Bravo et al., 2011b). It is worth noting, that the HFEs studied here may contribute more to the warming than expected from their direct GWP values due the cumulative effect of fluorinated esters formed during their atmospheric oxidation. To shed light on the

contribution to the warming of these oxidation products, we have theoretically estimated their radiative behavior (see Table S3, Supporting information for details). In this sense, we estimated a RE value of 0.58 W m^{-2} $ppbv^{-1}$ for the fluorinated formate coming from the HFE-7300 oxidation, what led to an indirect and net GWP_{100} of 310 and 750, respectively. For the fluorinated acetate and formate coming from HFE-7500 we predicted REs of 0.68 and 0.61 W m^{-2} $ppbv^{-1}$, respectively; and our estimated indirect and net GWP_{100} for HFE-7500 are 110 and 125. From this outlook we clearly see as the contribution to the warming of HFE-7300 and HFE-7500 may increase within 70–80% when we take into account this cumulative effect from the oxidation products when compare to the direct GWP estimations.

Acknowledgments

We thank the Spanish Ministry of Science – Education (CGL2011-24799) and the Castilla-La Mancha Science – Education Council (PEII09-0262-2753) for their financial support.

Appendix A. Supplementary data

Supplementary data related to this article can be found at http://dx.doi.org/10.1016/j.atmosenv.2014.07.033.

References

Aranda, A., Diaz-de-Mera, Y., Bravo, I., Rodriguez, D., Rodríguez, A., Martínez, E., 2006. Environ. Sci. Technol. 40, 5971–5976.
Atkinson, R., Baulch, D., Cox, R., Crowley, J.N., Hampson, R., Hynes, R., Jenkin, M., Rossi, M., Troe, J., 2006. Atmos. Chem. Phys. 6, 3625–4055.
Atkinson, R., Baulch, D., Cox, R., Crowley, J.N., Hampson, R., Hynes, R., Jenkin, M., Rossi, M., Troe, J., Wallington, T.J., 2008. Atmos. Chem. Phys. 8, 4141–4496.
Blanco, M.B., Bejan, I., Barnes, I., Wiesen, P., Teruel, A.M., 2012. Environ. Sci. Technol. 46, 8817–8825.
Blowers, P., Moline, D.M., Tetrault, K.F., Wheeler, R.R., Tuchawena, S.L., 2007. J. Geophys. Res. 112, D15108.
Bonard, A., Daele, V., Delfau, J.L., Vovelle, C., 2002. J. Phys. Chem. A 106, 4384–4389.
Bravo, I., Díaz-de-Mera, Y., Aranda, A., Smith, K., Shine, K.P., Marston, G., 2010a. Phys. Chem. Chem. Phys. 12, 5115–5125.
Bravo, I., Aranda, M.D., Hurley, G., Marston, D.R., Nutt, K.P., Shine, K., Smith, Wallington, T.J., 2010b. J. Geophys. Res. 115, D24317.
Bravo, I., Marston, G., Nutt, D.R., Shine, K.P., 2011a. J. Quant. Spectrosc. Radiat. Transf. 112, 1967–1977.
Bravo, I., Díaz-de-Mera, Y., Aranda, A., Moreno, E., Nutt, D.R., Marston, G., 2011b. Phys. Chem. Chem. Phys. 13, 17185–17193.
Bravo, I., Rodríguez, A., Rodríguez, D., Diaz-de-Mera, Y., Notario, A., Aranda, A., 2013. ChemPhysChem 14, 3834–3842.
Chen, L., Kutsuna, S., Nohara, K., Takeuchi, K., Ibusuki, T., 2001. J. Phys. Chem. A 105, 10854–10859.
Christense, L.K., Sehested, J., Nielsen, O.J., Bilde, M., Wallington, T.J., Guschin, A., Molina, L.T., Molina, M.J., 1998. J. Phys. Chem. A 102, 4839–4845.
Christensen, L.K., Wallington, T.J., Guschin, A., Hurley, M.D., 1999. J. Phys. Chem. A. 103, 4202–4208.
Cohen, N., Westberg, K.R., 1991. J. Phys. Chem. Ref. Data 20, 1211–1311.
Diaz-de-Mera, Y., Aranda, A., Bravo, I., Rodríguez, D., Rodríguez, A., Moreno, E., 2008. Environ. Sci. Pollut. Res. 15, 584–591.
Díaz-de-Mera, Y., Aranda, A., Bravo, I., Moreno, E., Martínez, E., Rodríguez, A., 2009. Chem. Phys. Lett. 479, 20–24.
Farman, J.D., Gardiner, B.G., Shanklin, J.D., 1985. Nature 315, 207–210.
Finlayson-Pitts, B.J., Pitts Jr., J.N., 2000. Chemistry of the Upper and Lower Atmosphere: Theory, Experiments, and Applications. Academic Press, San Diego, CA.
Forster, P.M.D., Ramaswamy, V., Artaxo, P., Berntsen, T., Betts, R., Fahey, D.W., Haywood, J., Lean, J., Lowe, D.C., Myhre, G., Nganga, J., Prinn, R., Raga, G., Schulz, M., Van Dorland, R., 2007. In: Solomon, S. (Ed.), Fourth Assessment Report of the Intergovernmental Panel on Climate Change. Cambridge.
Goto, M., Inoue, Y., Kawasaki, M., Guschin, A.G., Molina, L.T., Molina, M.J., Wallington, T.J., Hurley, M.D., 2002. Environ. Sci. Technol. 36, 2395–2402.
Hodnebrog, Ø., Etminan, M., Fuglestvedt, J.S., Marston, G., Myhre, G., Nielsen, C.J., Shine, K.P., Wallington, T.J., 2013. Rev. Geophys. 51, 300–378.
Hurley, M.D., Wallington, T.J., Laursen, L., Javadi, M.S., Nielsen, O.J., Yamanaka, T., Kawasaki, M., 2009. J. Phys. Chem. A. 113, 7011–7020.
Kaiser, E.W., Wallington, T.J., 1996. J. Phys. Chem. A. 100, 4111–4119.
Kurylo, M.J., Orkin, V.L., 2003. Chem. Rev. 103, 5049–5076.
Mellouki, A., Teton, S., LeBras, G., 1995. Int. J. Chem. Kinet. 27, 791–805.
Mielke, L.H., Furgeson, A., Osthoff, H.D., 2011. Environ. Sci. Technol. 45 (20), 8889–8896.
Molina, M.J., Rowland, F.S., 1974. Nature 249, 810–812.
Nohara, K., Toma, M., Kutsuna, S., Takeuchi, K., Ibusuki, T., 2001. Environ. Sci. Technol. 35, 114–120.
Notario, A., Mellouki, A., Le Bras, G., 2000. Int. J. Chem. Kinet. 32, 105–110.
Osthoff, H.D., Roberts, J.M., Ravishankara, A.R., Williams, E.J., Lerner, B.M., Sommariva, R., Bates, T.S., Coffman, D., Quinn, P.K., Dibb, J.E., Stark, H., Burkholder, J.B., Talukdar, R.K., Meagher, J., Fehsenfeld, F.C., Brown, S.S., 2008. Nat. Geosci. 1 (5), 324–328.
3M™ Novec™ 7500 Engineered Fluid, Product Information and 3M™ Novec™ 7300 Engineered Fluid, Product Information.
Oyaro, N., Nielsen, C.J., 2003. Asian Chem. Lett. 7, 119–122.
Oyaro, N., Sellevaag, S.R., Nielsen, C.J., 2005. J. Phys. Chem. A. 109, 337–346.
Papadimitrou, V.C., Kambanis, K.G., Lazarou, Y.G., Papagiannakopoulos, P., 2004. J. Phys. Chem. A 108, 2666–2674.
Phillips, G.J., Tang, M.J., Thieser, J., Brickwedde, B., Schuster, G., Bohn, B., Lelieveld, J., Crowley, J.N., 2012. Geophys. Res. Lett. 39, L10811.
Pinnock, S., Hurley, M.D., Shine, K.P., Wallington, T.J., Smyth, T.J., 1995. J. Geophys. Res. 100, 23227–23238.
Prinn, R.G., Huang, J., Weiss, R.F., Cunnold, D.M., Fraser, P.J., Simmonds, P.G., McCulloch, A., Harth, C., Salamch, P., O'Doherty, S., Wang, R.H.J., Porter, L., Miller, B.R., 2001. Science 292, 1882–1888.
Rodríguez, A., Rodríguez, D., Garzón, A., Soto, A., Aranda, A., Notario, A., 2010. Phys. Chem. Chem. Phys. 12, 12245–12258.
Rudolph, J., Hoppman, R., Plass-Dülmer, C.H., 1996. Atmos. Environ. 30, 1887–1894.
Sander, S.J., Abbatt, J.P.D., Barker, J.R., Burkholder, J.B., Friedl, R.R., Golden, D.M., Huie, R.E., Kolb, C.E., Kurylo, M.J., Moortgat, G.K., Orkin, V.L., Wine, P.H., 2011. Chemical Kinetics and Photochemical Data for Use in Atmospheric Studies, Evaluation No. 17. JPL Publication 10-6. Jet Propulsion Laboratory, Pasadena. http://jpldataeval.jpl.nasa.gov.
Scanlon, J.T., Willis, D.E., 1985. J. Chromatogr. Sci. 23, 333–340.
Spivakovsky, C.M., Logan, J.A., Montzka, S.A., Balkanski, Y.J., Foreman-Fowler, M., Jones, D.B.A., Horowitz, L.W., Fusco, A.C., Brenninkmeijer, C.A.M., Prather, M.J., Wofsy, S.C., McElroy, M.B., 2000. J. Geophys. Res. 105, 8931–8980.
Stein, S.E., Rukkers, J.M., Brown, R.L., 1991. NIST Standard Reference Database 25: Structures and Properties. NIST, Gaithersburg, MD.
Teton, S., Mellouki, A., LeBras, G., Sidebottom, H., 1995. Int. J. Chem. Kinet. 28, 291–297.
Teton, S., Mellouki, A., LeBras, G., Sidebottom, H., 1996. Int. J. Chem. Kinet. 28, 291–297.
Thornton, J.A., Kercher, J.P., Riedel, T.P., Wagner, N.L., Cozic, J., Holloway, J.S., Dubé, W.P., Wolfe, G.M., Quinn, P.K., Middlebrook, A.M., Alexander, B., Brown, S.S., 2010. Nature 464 (7286), 271–274.
Tokuhashi, K., Nagai, H., Takahashi, A., Kaise, M., Kondo, S., Sekiya, A., Takahashi, M., Gotoh, Y., Suga, S., 1999. J. Phys. Chem. A 103, 2664–2672.
Tsai, W.T., 2005. J. Hazard. Mater. A 119, 69–78.
WMO, 2011. Scientific Assessment of Ozone Depletion: 2010, Global Ozone Research and Monitoring Project – Report No. 50. World Meteorological Organization, Geneva, Switzerland, p. 572 (Rep).